Single Prime hAd5 Spike (S) + Nucleocapsid (N) Dual Antigen Vaccination of Healthy Volunteers Induces a Ten-Fold Increase in Mean S- and N- T-Cell Responses Equivalent to T-Cell Responses from Patients Previously Infected with SARS-CoV-2

Peter Sieling[1], Thomas King[1], Raymond Wong[1], Andy Nguyen[1], Kamil Wnuk[1], Elizabeth Gabitzsch[1], Adrian Rice[1], Helty Adisetiyo[1], Melanie Hermreck[1], Mohit Verma[1], Lise Zakin[1], Annie Shin[1], Brett Morimoto[1], Wendy Higashide[1], Kyle Dinkins[1], Joseph Balint[1], Victor Peykov[1], Justin Taft[2,3], Roosheel Patel[2,3], Sofija Buta[2,3,4], Marta Martin-Fernandez[2,3,4,5,6], Dusan Bogunovic[2,3,4,5,6], Patricia Spilman[1], Lennie Sender[7], Sandeep Reddy[7], Philip Robinson[8], Shahrooz Rabizadeh[1], Kayvan Niazi[1], and Patrick Soon-Shiong[1*]

Affiliations

[1]ImmunityBio, LLC, 9920 Jefferson Blvd., Culver City, CA 90232, USA

[2]Center for Inborn Errors of Immunity, [3]Department of Pediatrics, [4]Precision Immunology Institute, [5]Mindich Child Health and Development Institute, [6]Department of Microbiology, Icahn School of Medicine at Mount Sinai, 1 Gustave Lane, Levy Place, New York, NY 10029-5674, USA SPA

[7]NantKwest, Inc., 9920 Jefferson Blvd., Culver City, CA 90232, USA

[8]Hoag Hospital, Newport Beach, CA 92663, USA

*Corresponding author: Patrick@Nantworks.com

ABSTRACT

In response to the need for a safe, efficacious vaccine that provides broad immune protection against SARS-CoV-2 infection, we have developed a dual-antigen COVID-19 vaccine. The vaccine delivers both the viral spike (S) protein modified to increase cell-surface expression (S-Fusion) and the viral nucleocapsid (N) protein with an Enhanced T-cell Stimulation Domain (N-ETSD) to enhance MHC class I and II presentation and T-cell responses. The vaccine antigens are delivered using a human adenovirus serotype 5 (hAd5) platform with E1, E2b, and E3 regions deleted that has been shown in previous cancer vaccine studies to be effective in the presence of pre-existing hAd5 immunity. Here, we demonstrate the hAd5 S-Fusion + N-ETSD (hAd5 S + N) vaccine antigens when expressed by dendritic cells (DCs) of previously SARS-CoV-2-infected patients elicit Th1 dominant activation of autologous patient T cells, indicating the vaccine antigens have the potential for generating immune responses in patients previously infected or vaccinated. We further demonstrate that participants in our open-label Phase 1b study of the dual-antigen hAd5 S + N vaccine generate Th1 dominant S- and N- specific T cells after a single prime subcutaneous injection and that the magnitude of these responses were comparable to those seen for T cells from previously infected patients. We further present our *in silico* prediction of T-cell epitope HLA binding for both the first-wave SARS-CoV-2 'A' strain and the K417N, E484K, and N501Y S as well as the T201I N variants that suggests T-cell responses to the hAd5 S + N vaccine will retain efficacy against these variants. These findings that the dual-antigen hAd5 S + N vaccine elicits SARS-CoV-2-relevant T-cell responses and that such cell-mediated protection is likely to be sustained against emerging variants supports the testing of this vaccine as a universal booster that would enhance and broaden existing immune protection conferred by currently approved S-based vaccines.

50 **INTRODUCTION**

51 To address the need for an efficacious COVID-19 vaccine that elicits broad immunity against
52 SARS-CoV-2, is suitable for global distribution and use, and has a high likelihood of maintaining
53 efficacy against emerging SARS-CoV-2 variants, we have developed a dual-antigen COVID-19
54 'T cell' vaccine. This dual-antigen vaccine expresses both the virus spike (S) and nucleocapsid (N)
55 proteins using a next-generation human adenovirus serotype 5 (Ad5) platform. The S antigen is
56 full-length S including SD1 receptor binding domain, S1 and S2 domains modified to enhance
57 surface expression (S-Fusion); [1] and full-length N protein modified with an Enhanced T cell
58 Stimulation Domain (ETSD) to direct N to the endo-/lysosomal compartment for increased MHC
59 class I and II expression. The hAd5 platform used has deletions in the E1, E2b, and E3 gene
60 regions, thereby minimizing host anti-vector immune responses [2,3] and enabling efficient antigen
61 cargo expression and cognate T cell activation even in the presence of existing anti-adenovirus
62 immunity, as demonstrated previously in clinical studies targeting tumor-associated antigens in
63 cancer patients. [4,5]

64 The emergence of SARS-CoV-2 variants that have the potential to evade immune responses
65 generated in response to currently available vaccines has spurred renewed interest in the potential
66 role of T cells in conferring long-term protection against COVID-19. [6-9] SARS-CoV-2 vaccine
67 development has focused largely on eliciting neutralizing antibodies against the S protein to inhibit
68 infection and reduce disease severity. [10-14] S-specific T cell responses have been reported for two
69 available vaccines, mRNA1273 and BNT162b1, [15,16] however, their role in conferring protective
70 immunity against COVID-19 is unclear.

71 SARS-CoV-2 strain analysis in participants in Phase 3 studies in South Africa has revealed
72 that some vaccines show diminished protection against the B.1.351 variant strain, [17] including
73 ChAdOx, [18] NVX-CoV2373, [19,20] and Ad26.COV2-S. [21] In addition, *in vitro* studies show that wild
74 type S-specific antibodies elicited by mRNA-1273 and BNT162b1 show reduced binding to the

75 B.1.351 variant S protein. [22-24] Taken together, these findings raise the concern that monovalent
76 vaccines targeting only the S protein may not be the most optimal strategy for conferring protection
77 against continually emerging variants.

78 SARS-CoV-2 expresses a number of other immunogenic proteins that may induce protective
79 antibody and/or T cell responses. Among these, the N protein is the most abundantly expressed, is
80 highly conserved among coronaviruses, and has been studied previously as an antigen for
81 therapeutics and vaccines for SARS-CoV.[25-29] Inclusion of N-derived antigens into vaccine
82 designs may be a rational strategy to elicit broader protective immunity against SARS-CoV-2 with
83 a high probability of being sustained against variants. The N protein associates with viral RNA
84 within the SARS-CoV-2 virion and is necessary for viral RNA replication, virion assembly, and
85 release from host cells.[28,29] Virtually all SARS-CoV-2 convalescents develop N-specific antibody
86 and $CD8^+$ and/or $CD4^+$ T cell responses.[30] Remarkably, SARS-CoV convalescents from 2003
87 maintain robust cognate N-specific $CD8^+$ and/or $CD4^+$ T cell responses that were detectable up to
88 17 years later.[31] These long-lived memory T cells also cross-react with N and other proteins of
89 SARS-CoV-2.[31] To a lesser extent, individuals with no history of exposure to SARS-CoV, SARS-
90 CoV-2, or Middle Eastern Respiratory Syndrome (MERS) also show cross-reactive SARS-CoV-
91 2 N-specific $CD8^+$ and/or $CD4^+$ T cell responses, likely due to prior exposure to related endemic
92 coronaviruses including OC43, HKU1, 229E, and NL63.[30] These data suggest that induction of
93 N-specific memory T cell responses via vaccination may at least partly recapitulate the natural
94 course of SARS-CoV-2 infection and recovery from illness, and could be beneficial for achieving
95 more optimal disease-limiting immunity against the virus.

96 Our addition of N to our dual antigen hAd5 S-Fusion + N-ETSD vaccine leverages the ability
97 to N to generate protective, durable T-cell responses. Recent characterization of COVID-19 patient
98 immune responses to SARS-CoV-2 indicates T cell activation is critical for clearance of infection
99 and production of long-term immunity to coronavirus infections.[31-34] Both CD4+ and CD8+ T cells

100 underpin durable humoral responses because CD4+ T cells, while not effector cells like CD8+ T
101 cells, are critical to the generation of robust and long-lasting immunity afforded by antibody-
102 secreting plasma cells and the elimination of infected cells by memory cytotoxic CD8+ T cells.[35,36]
103 In the studies reported here, we first confirm that the addition of the ETSD to N, intended to
104 increase MHC class I and II responses and T-cell activation, directs N to the cell endo-/lysosomal
105 compartment. We then demonstrate that the hAd5-S-Fusion + N-ETSD COVID-19 vaccine
106 antigens, when expressed by monocyte-derived dendritic cells (MoDCs) from individuals
107 previously infected with SARS-CoV-2, can activate and induce recall of S- and N-specific
108 autologous $CD8^+$ and $CD4^+$ T cells. We specifically show that overall, N-ETSD elicits greater T-
109 cell responses than N without the ETSD. This study demonstrates the vaccine-expressed antigens
110 are 'recalled' by T cells and thus suggests they have the potential to induce relevant, protective
111 immune responses in previously SARS-CoV-2 infected or vaccinated individuals who receive the
112 hAd5 S-Fusion + N-ETSD vaccine.
113 We next show that T cells isolated 14 and 23 days after prime vaccination alone from
114 participants in our ongoing Phase 1b clinical trials of the hAd5 S-Fusion + N-ETSD vaccine are
115 activated by both S and N peptides pools and that these T-cell responses are comparable in
116 magnitude to those of T cells from previously SARS-CoV-2 infected patients.
117 To support our proposition that a 'T cell' vaccine that provides both S and N antigens will
118 sustain efficacy against variants, we also present our *in silico* prediction of T cell epitope HLA
119 binding based on analyses of all possible 9-mer epitopes from both first-wave 'A' strain SARS-
120 CoV-2 and the variants that are found in the B.1.351 strain discovered in South Africa – spike
121 K417N, E484K, and N501Y and nucleocapsid T205I. This analysis shows that memory T-cell-
122 mediated immunity has a very low probability of being significantly affected by the B.1.351
123 variants and that the hAd5 S + N COVID-19 T-cell vaccine has the potential of being protective
124 against these variants.

125 **RESULTS**

126 ***N-ETSD is directed to endo-/lysosomal and autophagosomal compartments***

127 The hAd5 dual antigen vaccine construct includes sequences designed to target N to MHC
128 class II antigen loading compartments. To confirm this occurs, we evaluated the localization of N-
129 ETSD in human monocyte-derived dendritic cells (MoDCs) compared to its untargeted
130 cytoplasmic counterpart (N). MoDCs from healthy subjects were infected with hAd5 N-ETSD or
131 hAd5 N and localization was determined by immunocytochemistry. N-ETSD showed localization
132 to discrete vesicles, some coincident with CD71, a marker of recycling endosomes (Fig. 1A-C),
133 and LAMP-1, a marker for late endosome/lysosomes (Fig. 1G-I), whereas N was expressed
134 diffusely and uniformly throughout the cytoplasm (Fig. 1D-F; J-L).

135 Studies have shown that lysosomes fuse with autophagosomes to enhance peptide processing
136 and MHC class II presentation.[37,38] Thus we examined whether N-ETSD localized in
137 autophagosomes in MoDCs by co-labeling with the autophagosome marker LC3a/b [39] to identify
138 another potential site of localization relevant to MHC class II antigen presentation.[40] We found
139 that N-ETSD also displayed some co-localization with the autophagosome marker (Fig. 1M-O).

140 Protein processing in autophagosomes plays a key role in MHC-mediated antigen presentation
141 in DCs,[41-43] providing a potential mechanism of enhanced CD4+ T cells induced by N-ETSD in
142 the vaccine construct. Evidence of this T cell interaction with a MoDC infected with N-ETSD
143 translocated to autophagosomes (and, it is assumed, also endosomes and lysosomes) is seen in this
144 phase-contrast microscopy of the N-ETSD and LC3a/b co-labeled cells, which reveals the
145 elongated DC morphology in contrast to the spherical morphology of what are posited to be
146 undifferentiated lymphocytes.

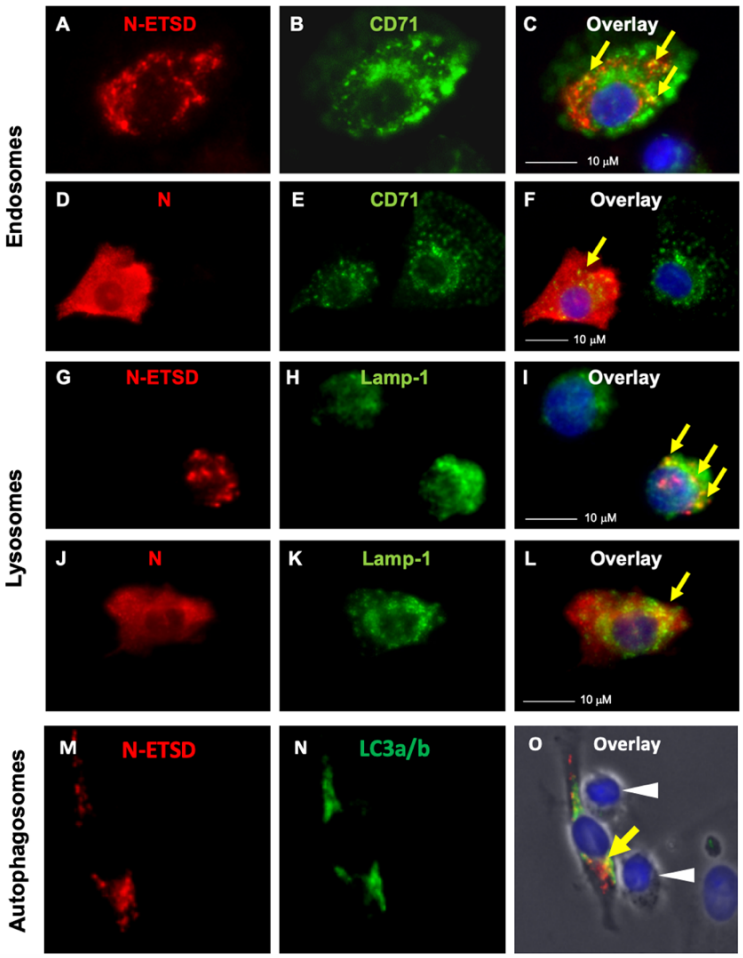

Fig. 1 *N-ETSD localizes to endosomes, lysosomes, and autophagosomes.* MoDCs were infected with Ad5 N-ETSD or N without ETSD and were co-labeled with anti-flag (N, N-ETSD here have a flag tag) and anti-CD71 (endosomal marker), anti-Lamp 1 (lysosomal marker), or anti-LC3a/b antibodies. (A) N-ETSD, (B) CD71, and (C) overlay. (D) N, (E) CD71, and (F) overlay. (G) N-ETSD, (H) Lamp-1, and (I) overlay. (J) N, (K) Lamp-1, and (L) overlay. (M) N-ETSD, (N) LC3a/b, and (O) overlay. N/N-ETSD is red, other markers green, co-localization indicated by yellow arrows, and white arrows indicate suspected undifferentiated lymphocytes.

The Immune Recall Study with Previously SARS-CoV-2 Infected Patients

Blood samples from previously SARS-CoV-2 infected patients confirmed to show humoral and T-cell responses and enhanced binding to hAd5 S-Fusion + N-ETSD expressing cells

For the 'recall' studies described below, plasma samples were collected from four individuals convalescing from SARS-CoV-2 infection as confirmed by antibody assays and patient history. The presence of anti-Spike IgG, and neutralizing antibodies by both a surrogate SARS-CoV-1 neutralization [44] and live virus assays, were confirmed in all patient samples (Suppl. Fig. S1). Samples from four virus-naïve individuals were used as controls.

164 In additional studies to validate immune responses to SARS-CoV-2 antigens, the binding of
165 previously SARS-CoV-2 infected patient and virus-naïve control individual plasma to human
166 embryonic kidney (HEK) 293T cells transfected with either hAd5 S-Fusion alone or hAd5 S-
167 Fusion + N-ETSD was assessed (Suppl. Fig. S2). This binding reflects the presence of antibodies
168 in plasma that recognize antigens expressed by the hAd5 vectored vaccines. Quantification of
169 histograms showed little or no binding of virus-naïve plasma antibodies to cells expressing
170 constructs, with the highest previously SARS-CoV-2 infected patient plasma binding to cells
171 expressing the dual antigen S-Fusion + N-ETSD construct (Suppl. Fig. S2R).

172 To confirm the T cells from previously SARS-CoV-2-infected patients were reactive to
173 SARS-CoV-2 peptides, isolated T cells from the patients were incubated with S1 (containing the
174 S receptor binding domain), S2 and N peptides pools. T cells from all four patients showed
175 reactivity (Suppl. Fig. S3). Selected CD4+ and CD8+ T cells from 2 patients were activated by S1,
176 S2, and N peptides, revealing CD8+ T cells were more reactive to N (Suppl. Fig. S3D and E).

177 ***Previously SARS-CoV-2 infected patient Th1 dominant CD3+ and CD4+/CD8+ memory T-cells***
178 ***recall N-ETSD antigens expressed by autologous hAd5-infected MoDCs***

179 To evaluate the immune significance of endo/lysosome-localized N-ETSD versus cytoplasmic
180 N, MoDCs were infected with hAd5 constructs (Null, N-ETSD or N) then incubated with
181 autologous CD3+ and CD4+- or CD8+-selected T cells (Fig. 2A). CD3+ T cells from previously
182 infected SARS-CoV-2 patients showed significantly greater IFN-γ secretion in response to N-
183 ETSD than both Null and cytoplasmic N in the two patients where N-ETSD and N were compared
184 (Fig. 2C and D). There were relatively few interleukin-4 (IL-4) secreting CD3+ T cells for all
185 patients (Fig. 2E-G); the high IFN-γ and low IL-4 responses show Th1 dominance for both N-
186 ETSD and N. Both CD4+ and CD8+ selected T-cell populations showed significantly greater IFN-

γ responses to N-ETSD than Null (Fig. 2H-M) and in two of three patients, CD4+ and CD8+ T cells showed greater recognition of N-ETSD compared to N.

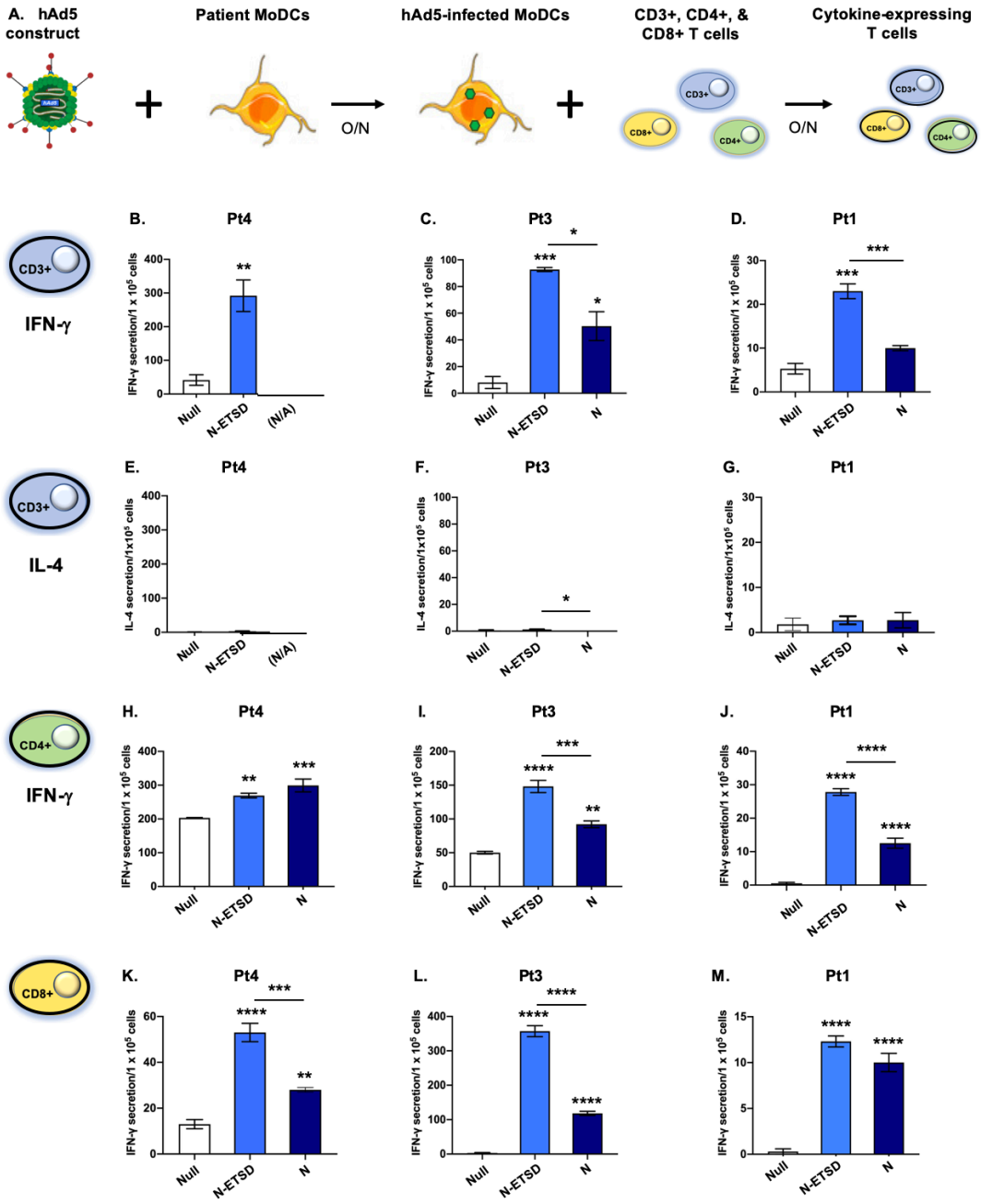

Fig. 2 *Previously SARS-CoV-2 infected patient T-cell IFN-γ secretion is greater in response to MoDC-expressed N-ETSD than N and is Th1 dominant*. (A) Experimental design. Secretion of IFN-γ (B-D) or interleukin-4 (E-G) by autologous CD3+ T cells in response to hAd5 N-ETSD-/N-/Null- expressing MoDCs is shown (same scale for IFN-γ and IL-4 for each Pt). IFN-γ secretion by CD4+ (H-J) and CD8+ (K-M) T cells in response to hAd5-N-ETSD/N/Null are shown. Statistical analysis performed using One-way ANOVA and Tukey's post-hoc multiple comparison analysis, where *p<=0.05; **p<0.01, ***p<0.001 and ****p<0.0001. Comparison to Null shown above bars, comparison between N-ETSD and N indicated with a line. Data graphed as mean and SEM; n = 3-4.

199 ***CD4+ and CD8+ memory T-cells from previously SARS-CoV-2 infected patients recall***
200 ***nucleocapsid and spike antigens expressed by autologous hAd5-infected MoDCs***

201 To compare CD3+, CD4+, CD8+ memory T-cell responses to the components of the hAd5 S-
202 Fusion + N-ETSD vaccine, MoDCs were infected with hAd5 S-Fusion, hAd5 N-ETSD, or the dual
203 antigen vaccine (Fig. 3A).

204 For unselected CD3+ T cells, IFN-γ responses were similar to S-Fusion + N-ETSD and N-
205 ETSD with responses to S-Fusion being relatively low (Fig. 3A-C). The number of IL-4 secreting
206 T cells in response to any infected MoDC was very low (Fig. 3D-F). Based on the increased
207 expression of S in the dual antigen vaccine compared to monovalent S-Fusion, the increased T-
208 cell responses could be explained by either T cells recognizing increased S or the presence of N.
209 Importantly, these T-cell responses were characterized by a predominance of IFN-γ (Th1) relative
210 to IL-4 (Th2).

211 CD4+ T cells from all three patients showed significantly greater recognition of all three
212 constructs compared to Null (Fig. 3G-I). While there were greater responses to specific constructs
213 in some individuals, overall the responses to S-Fusion, S-Fusion + N-ETSD and N-ETSD were
214 similar. CD8+ T cells from all three patients recognized the dual antigen and N-ETSD vaccines at
215 a significantly higher level than Null; in only two of three patients did CD8+T cells recognize S-
216 Fusion to a significant degree above Null (Fig. 3J-L). These data indicate that T cells from
217 previously infected SARS-CoV-2 patients have reactivity and immune memory recall to both of
218 the vaccine antigens (S and N) in our vaccine vector.

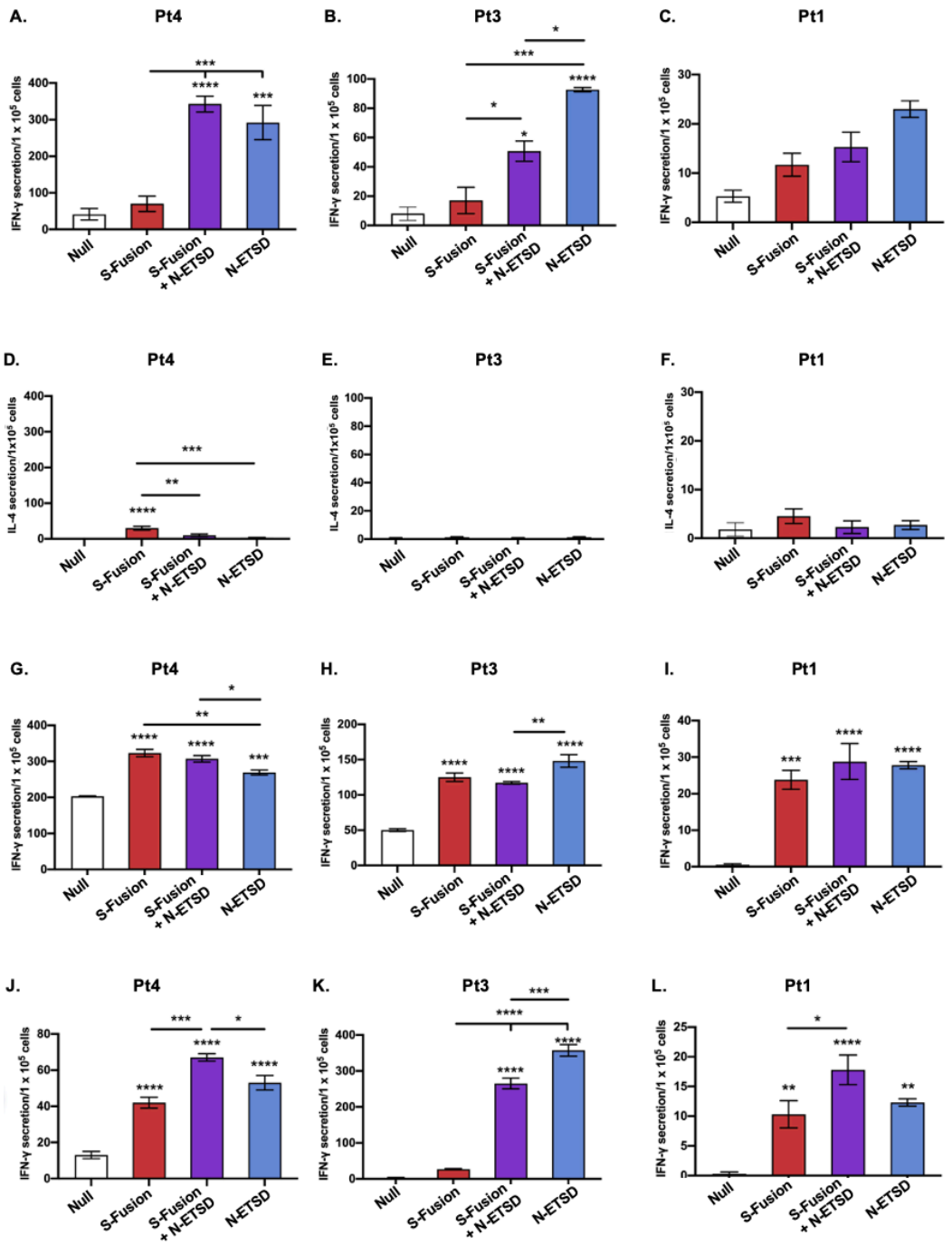

Fig. 3 *Previously SARS-CoV-2 infected patient T-cell responses to the dual antigen vaccine and its individual components reveal distinct antigen specificity of T-cell populations.* (A-C) CD3+ T cell IFN-γ responses for three patients. (D-F) CD3+ T cell IL-4 responses. (G-I) CD4+ IFN-γ responses. (J-L) CD8+ IFN-γ responses. Statistical analysis performed using One-way ANOVA and Tukey's post-hoc multiple comparison analysis to compared each antigen-containing construct to the Null construct, where *$p<0.05$ and ****$p<0.00001$. Comparison to Null only above bars; comparison between antigen-expressing vaccines above lines. Data graphed as mean and SEM; n = 3-4.

230 **T-Cell Responses after a Single Prime Vaccination in a Phase 1 Clinical Trial**

231 For the ELISpot assay results shown here, T cells were isolated from patients in cohort 2 of
232 the Phase 1b study of the ImmunityBio hAd5 COVID-19 'T cell' vaccine (NCT04591717). These
233 participants were vaccinated subcutaneously with $1x10^{11}$ hAd5 S-Fusion + N-ETSD viral particles
234 (VP).

235 The studies presented here are experimental and all assays and analyses were performed in-
236 house at ImmunityBio, Inc. Formal analyses of the primary and secondary end points are ongoing
237 pending completion of the trial.

238 ***T cells from vaccinated participants show Th1 dominant responses to S and N by Day 14 after***
239 ***a single prime injection, with a more than 10-fold increase in mean responses to N***

240 T-cell responses to S, N, and SARS-CoV-2 membrane (M) peptides were determined by
241 ELISpot for clinical study participants pre-vaccination (Day 1) and at two time points following
242 the prime injection: Days 14-16 and 21-23.

243 By Day 14-16, T-cell secretion of IFN-γ in response to N peptides increased more than 10-
244 fold compared to pre-vaccination (Day 1); these responses were sustained on Day 21-23 and were
245 significant (Fig. 4A). The changes in T-cell responses to N for individual participants from pre- to
246 post-vaccination are shown in Fig. 4B.

247 T-cell secretion of IFN-γ in response to S peptides also increased post-prime only vaccination,
248 increasing more than 3-fold by Day 14-16 and more than 10-fold by Day 21-23, when differences
249 were significant (Fig. 4C). T-cell responses to S for individual participants are shown in Fig. 4D.

250 When responses to S, N and SARS-CoV-2 membrane (M) peptides are compared, the greatest
251 responses are seen to N peptides (Fig. 4F and G). As expected, there were very low/no responses
252 to M peptide, not delivered in the vaccine. Importantly, IL-4 secretion in response to peptide
253 stimulation was very low, indicating all responses to vaccine antigens were highly Th1 dominant.

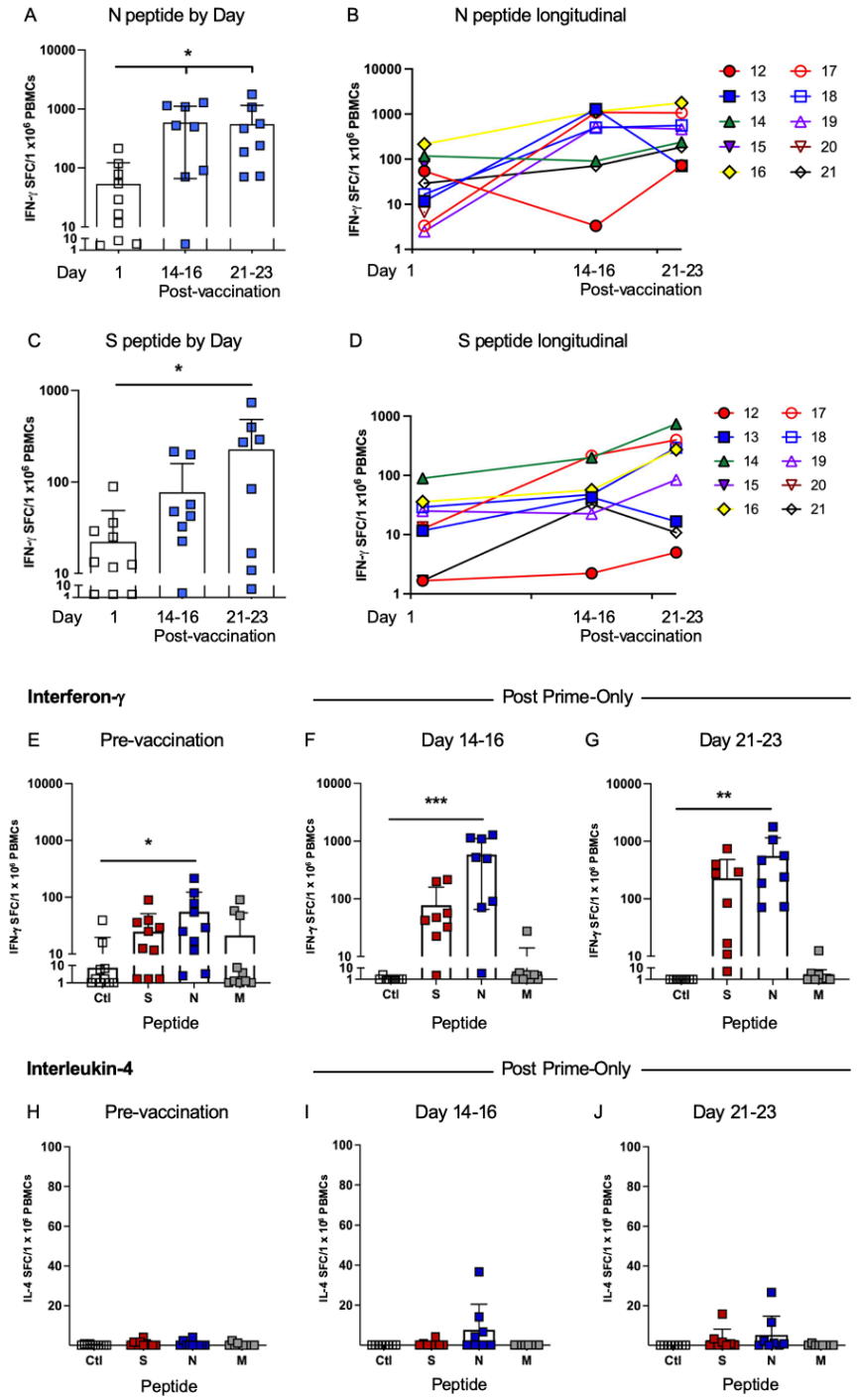

Fig. 4 *Vaccinated participant T-cell responses to S, N, and M peptides*. (A) T-cell interferon-γ (IFN-γ) secretion in response to nucleocapsid (N) peptide is shown for pre-vaccination (Day 1) and post-prime only Day 14-16 and 21-23. (B) Individual participant T-cell responses to N. (C)T-cell IFN-γ secretion in response to spike (S) peptide is shown for pre-vaccination (Day 1) and post-prime only Day 14-16 and 21-23. (D) Individual participant T-cell responses to S. T-cell IFN-γ secretion in response to no stimulation (Ctl), S, N and membrane (M) (E) pre-vaccination and on (F) Day 14-16 and (G) 21-23 post-prime only. (H-J) Interleukin-4 (IL-4) secretion. Statistical analysis performed using One-way ANOVA and Sidak's post-hoc analysis to compare pre-to post-vaccination (A, C) or peptide stimulation to Ctl (E-J), where *p , 0.05, **p ≤ 0.01, and ***p ≤ 0.001. Data graphed as mean and SD; baseline n = 9, Day 14-16 n = 7, Day 21-23 n = 8.

265 ***T-cell responses to S and N antigens generated from hAd5 prime vaccination alone were***
266 ***equivalent to those from previously SARS-CoV-2 infected patients***

267 As shown in Figure 5, T-cell responses to both N and S for previously SARS-CoV-2 infected
268 patients (Pt) and hAd5 S-Fusion + N-ETSD vaccinated participants (IB Vac) on Day 21-23 were
269 comparable. For responses to N, both Pt and IB Vac were ~40-fold greater than Unex; and for
270 responses to S, both Pt and IB Vac were >15-fold higher than Unex. As expected, T cells from
271 previously SARS-CoV-2 infected patients, but not vaccinated participants, reacted to M due to its
272 presence in the live virus. The M antigen is not present in the vaccine.

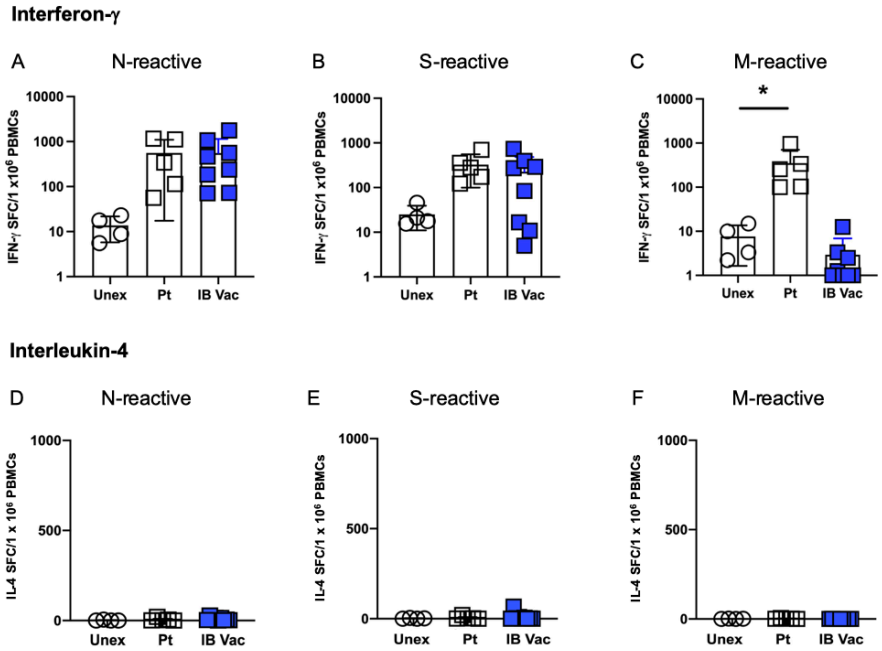

273
274 **Fig. 5** *T-cells from vaccinated and previously SARS-CoV-2 infected individuals show similar*
275 *responses to S and N.* T-cell secretion of interferon-γ (IFN-γ) in response to (A) N, (B) S, and (C)
276 M as determined by ELISpot shown for SARS-CoV-2 unexposed (Unex) and previously infected
277 (Pt) individuals as compared to participants receiving a prime vaccination alone (IB Vac) from
278 Day 21-23. Secretion of interleukin-4 (IL-4) in response to (D) N, (E) S, and (F) M. Statistical
279 analysis performed using One-Way ANOVA with Dunnett's post-hoc analysis comparing Pt and
280 IB Vac to Unex; for IFN-γ secretion in response to M, Pt compared to Unex, $p = 0.0303$. Data
281 graphed as mean and SEM; Unex n = 4, Pt n = 5, IB vac n = 8.
282
283

284

285

286 **T-Cell Epitope HLA Binding Prediction**

287 ***In silico identification of 9-mer T-cell epitopes and HLA binding prediction suggests this***
288 ***binding is not significantly affected by B.1.351 strain variants***

289 To understand and predict the possible effects emerging SARS-CoV-2 variants on vaccine-
290 elicited T-cell protection, we utilized our in-house T-cell epitope identification and binding
291 analysis pipeline to compare the first wave 'A' strain epitopes to emerging variant strains.

292 *In silico* epitope analysis of the reference strain assembled from 75,000 individual sequences
293 deposited in the GISAID database [45,52] revealed 2479 MHC class I and 20963 MHC class II
294 potential binders. Altogether, the SARS-CoV-2 variants (K417N, E484K and N501Y mutations)
295 generate 10970 MHC class I and 18017 MHC class II unique epitopes.

296 We compared these unique epitopes to the reference strain and counted the different epitopes
297 that are bound by HLAs, finding 1659 unique MHC class I and 2887 unique MHC class II epitopes
298 that only exist in the variants and not the original strain. These epitopes are from the S, envelope
299 (E), N and membrane (M) proteins, but the most unique epitopes were found in variant S due to
300 the higher numbers of coding mutations.

301 For HLA binding prediction, sequences and predicted binding are compared and aligned and
302 show that, for example, as compared to the 'A' strain, an B.1.351 sequence has a 3 amino acid
303 deletion that results in a unique sequence RFQTLHRSYL predicted to bind HLA-C*14:02. By
304 similar determination of the epitopes and HLAs from the reference strain and the variant strains,
305 were identified differences in binding affinity or HLAs. Similarly at the N501Y site, the reference
306 strain generates an epitope (TNGVGYQPY) predicted to bind HLA-A*30:02, while the B.1.351
307 strain would generate a different yet similar epitope (TYGVGYQPY) also predicted to bind HLA-
308 A*30:02.

309 The key questions asked here were: how does mutation change HLA availability and which
310 mutations favor immune evasion? Not all mutations lead to evasion; while a mutation may lead to

311 an amino acid substitution that has potential functional consequences, that same mutation may still
312 generate an epitope that retains HLA binding affinity and does not contribute to escape. The unique
313 binding HLAs for each S variants when compared to the A strain are shown in Figure 1. For class
314 I, there are only 2 K417N (B.1.351) HLAs and for the A strain there are 6 (Fig. 6A); for E484K
315 there are 8 and for the A strain 7 (Fig. 6B); and for N501Y there are 8 and only 1 for the A strain
316 (Fig. 6C). There are no unique class II HLAs for these same comparisons (Fig. 6D-F).
317 In the B.1.351 strain, there is only one N mutation – T205I. Similarly to the S variants, there
318 are few unique binding HLAs. For class I, the T201I mutation generates 2 and the A strain 3 unique
319 binding HLAs (Fig. 6G). For class II, the T205I generates 4 and the A strain just 1 unique binding
320 HLA(s) (Fig. 6H).

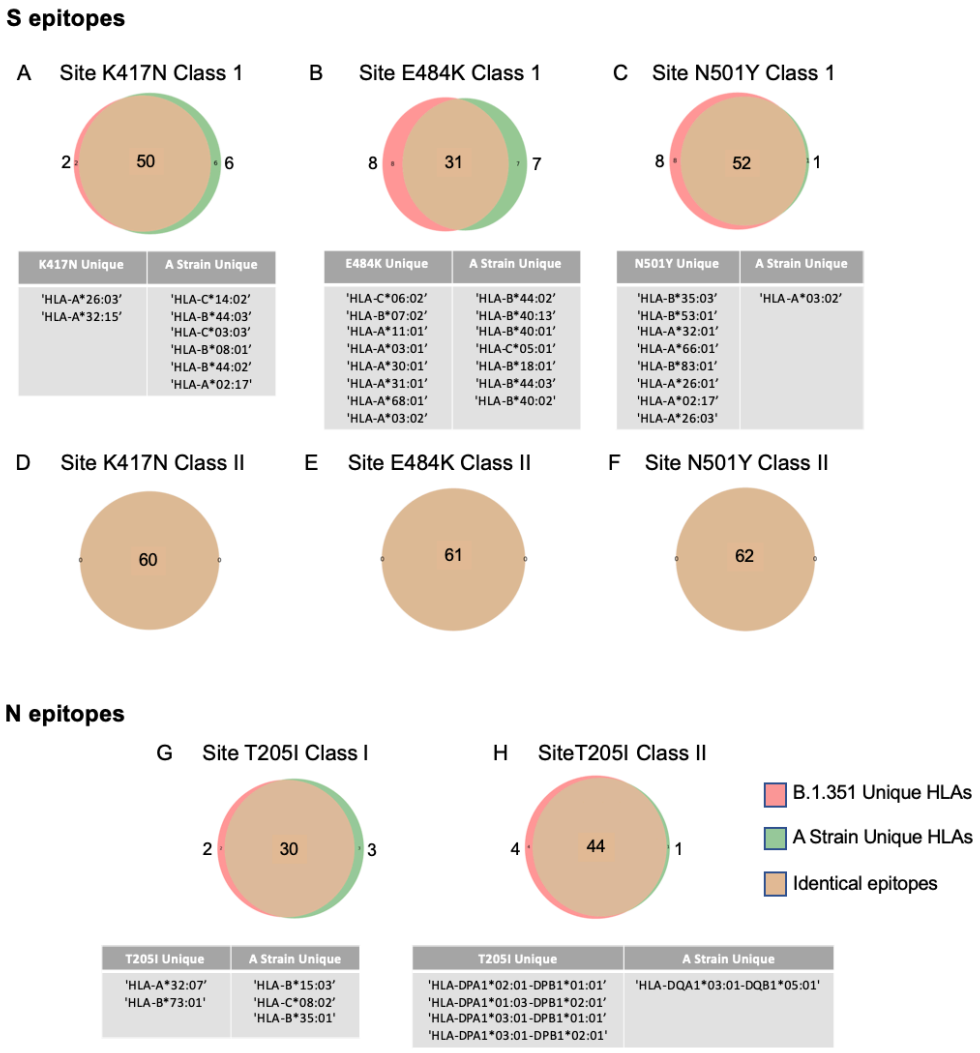

321

322 **Fig. 6** *A high degree of overlap is seen for HLA binding of predicted T-cell epitopes from variants*
323 *and the first-wave A strain SARS-CoV-2.* Comparison of 'A' and B.1.351 strain predicted class I
324 T-cell epitopes reveals significant overlap for the spike (A) K417N (50 of 58 epitopes), (B) E484K
325 (31 of 46 epitopes), and (C) N501Y (52 of 61 epitopes) variants. (D-F) Complete overlap is seen
326 for class II epitopes for those variants, respectively. (G) For T205I class I, 30 of 35 epitopes overlap
327 and (H) for class II, 44 of 49. Unique HLA class I binding is shown in the tables.
328

329 **DISCUSSION**

330 The emergence and rapid spread of SARS-CoV-2 variants is raising concern that first
331 generation monovalent wild-type S-targeting vaccines may eventually lose effectiveness at
332 protecting against COVID-19. In addition to updating S sequences to include variants in current
333 vaccines, alternate or complimentary vaccine strategies with enhanced focus on eliciting protective
334 T cell responses and possibly inclusion of other immunogenic structural proteins, including M
335 and/or N. Evidence indicates that virtually all COVID-19 convalescents develop IFN-γ-secreting
336 $CD4^+$ and/or $CD8^+$ T cell responses not only against S, but also against the M and N proteins of
337 SARS-CoV-2. [30] Significant T cell reactivity in COVID-19 convalescents has also been observed
338 against a wide breadth of other SARS-CoV-2 proteins, particularly nsp6 and ORF3a.[27,30,46]
339 Collectively, the total magnitude of the T cell response against non-S proteins such as N appears
340 at least equal to or possibly greater than the T cell response against S in COVID-19
341 convalescents.[27,30,46] Further, in a recent report by Redd *et al.* [7] the authors assessed reactivity of
342 CD8+ T cells from thirty COVID-19 convalescent individuals to forty-five different mutations and
343 concluded that virtually all CD8+ T cell responses to SARS-CoV-2 antigens should recognize the
344 variants. Taken together, these data suggest that monovalent S-targeting vaccines designed to elicit
345 humoral responses show a relatively narrow T cell response compared to the natural T cell
346 responses to N and other antigens observed in COVID-19 convalescents.

347 Here we show that our strategy of including N-ETSD, confirmed to be directed to the endo-
348 /lysosomal compartment with S optimized for cell-surface display [1,47] results in recognition of the
349 N-ETSD and S-Fusion + N-ETSD antigen(s) by previously SARS-CoV-2 patient T cells and in

350 generation of S- and N-reactive T cells in participants receiving the hAd5 S-Fusion + N-ETSD
351 vaccine. Not only does the enhancement of T-cell responses by the addition of N in this vaccine
352 confer a greatly likelihood of sustained protection against variants as our T-cell epitope HLA
353 binding prediction analysis would suggest, it presents the possibility that this vaccine can be
354 effective as a 'universal' booster. Not only would boosting with this vaccine likely increase cell-
355 mediated protection for individuals who have already received a first-generation S-only vaccine,
356 because the N protein is highly conserved among coronaviruses,[48] the hAd5-S-Fusion + N-ETSD
357 vaccine might provide protection against viruses similar to SARS-CoV-2 that may arise.
358 The hAd5 S-Fusion + N-ETSD COVID-19 T cell vaccine is currently undergoing clinical
359 testing with delivery by a variety of routes, including sublingual, SC, intranasal, and a thermally-
360 stable oral tablet as a prime/boost to provide protection against SARS-CoV-2. We anticipate our
361 testing its use as a universal boost for current first generation vaccines in the near future.
362

363 **ACKNOWLEDGEMENTS**

364 We thank the volunteers participating in our Phase I COVID-19 vaccine clinical trial and
365 Deborah Fridman, Director of Clinical Research at Hoag Hospital (Irvine/Newport Beach, CA).
366 We also thank Phil Yang of ImmunityBio for his ongoing coordination of project updates for the
367 studies described herein.
368

369 **MATERIALS and METHODS**

370 **Production hAd5-S-Fusion+N-ETSD and related SARS-CoV-2 antigen expressing vectors.**

371 Production of all hAd5 [E1-, E2b-, E3-] (Fig. 7A) constructs and virus particles were carried
372 out as previously described.[49] In brief, high titer adenoviral stocks were generated by serial
373 propagation in the E1- and E2b-expressing E.C7 packaging cell line, followed by $CsCl_2$
374 purification, and dialysis into storage buffer (2.5% glycerol, 20 mM Tris pH 8, 25 mM NaCl) by

375 ViraQuest Inc. (North Liberty, IA). Viral particle counts were determined by sodium dodecyl
376 sulfate disruption and spectrophotometry at 260 and 280 nm. Viral titers were determined using
377 the Adeno-X™ Rapid Titer Kit (Takara Bio).

378 The constructs created included:

379 B. S-Fusion: S optimized to enhance surface expression and display of RBD.

380 C. N (N without ETSD): Nucleocapsid (wild type) sequences with tags for immune detection, but
381 without ETSD modification, and predominantly cytoplasmic localization.

382 D. N with the Enhanced T cell Stimulation Domain (N-ETSD): Nucleocapsid (wild type) with
383 ETSD to direct lysosomal/endosomal localization and tags for immune detection.

384 E. The dual-antigen hAd5 S-Fusion + N-ETSD vaccine.

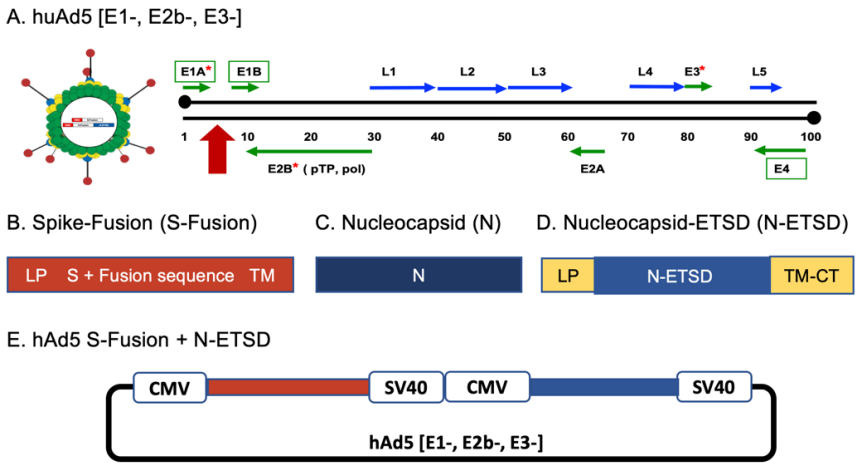

385
386 **Fig. 7** *Human adenovirus serotype 5 (hAd5) platform and constructs*. (A) hAd5 with E1, E2b and
387 E3 regions deleted (hAd5[E1-, E2b-, E3-]). The site of antigen sequence insertion is shown with a
388 red arrow. Constructs tested included (B) spike (S)-Fusion, (C) nucleocapsid (N) without the
389 Enhanced T-cell Stimulation Domain (ETSD), (D) N-ETSD, and (E) the hAd5 S-Fusion + N-
390 ETSD vaccine.
391

392 **The T-cell recall studies of unexposed and previously SARS-CoV-2 infected individuals**

393 *Collection of plasma and PBMCs for differentiation of MoDCs from patients with confirmed*
394 *previous SARS-CoV-2 infection and from virus-naïve volunteers*

395 Blood was collected with informed consent via venipuncture from volunteer patients (Pt) who
396 had either not been exposed (UNEX) to SARS-CoV-2 as confirmed by ELISA and multiple

397 negative SARS-CoV-2 tests or who had recovered from COVID-19 as indicated by recent medical
398 history and a positive SARS-CoV-2 antibody test. The presence of anti-S IgG and of neutralizing
399 antibodies in plasma from previously SARS-CoV-2 infected patients was confirmed by ELISA, a
400 surrogate neutralization assay,[44] and a live virus assay as shown in Supplementary Fig. S1. A third
401 source of whole blood was apheresis of healthy subjects from a commercial source (HemaCare).
402 Peripheral blood mononuclear cells (PBMCs) were isolated from whole blood by density
403 gradient centrifugation and plasma was collected after density gradient centrifugation.
404 Monocyte-derived dendritic cells (MoDC) were differentiated from PBMC using GM-CSF
405 (200U/ml) and IL-4 (100U/ml) as previously described [50]. Briefly, monocytes were enriched by
406 adherence on plastic, while the non-adherent cells were saved and frozen as a source of
407 lymphocytes, specifically T cells. Adherent cells were differentiated into dendritic cells (3-5 d in
408 RPMI containing 10% FBS), then frozen in liquid nitrogen for later use. T cells were enriched
409 from the non-adherent fraction of PBMC using MojoSort (BioLegend CD3 enrichment). CD4+
410 and CD8+ T cells were enriched using analogous kits from the same manufacturer. Efficiency of
411 the cell separations was evaluated by flow cytometry.
412 *Transduction of MoDCs with hAd5 N-WT or N-ETSD and labeling with anti-N, anti-CD71, anti-*
413 *LAMP-1, and Anti-LC3a/b antibodies*
414 Freshly thawed MoDCs were plated on 4-well Lab-Tek II CC2 Chamber Slides, using 3 x10^4
415 cells per well and transduction performed at MOI 5000 one hour after plating using hAd5 N-ETSD
416 or hAd5 N. Slides were incubated o/n at 37°C, fixed in 4% paraformaldehyde for 15 minutes, then
417 permeabilized with 1% Triton X100, in PBS) for 15 min. at room temperature. To label N, cells
418 were then incubated with an anti-flag monoclonal (Anti-Flag M2 produced in mouse) antibody at
419 1:1000 in phosphate buffered saline (PBS) with 3% BSA, 0.5% Triton X100 and 0.01% saponin
420 overnight at 4°C, followed by three washes in PBS and a 1 hour incubation with a goat anti-Mouse
421 IgG (H+L) Highly Cross-Adsorbed Secondary Antibody, Alexa Fluor Plus 555 (Life

422 Technologies) at 1:500. For co-localization studies, cells were also incubated overnight at 4°C with
423 a rabbit anti-CD71 (transferrin receptor, recycling/sorting endosomal marker) antibody
424 (ThermoFisher) at 1:200; sheep anti-Lamp1 Alexa Fluor 488-conjugated (lysosomal marker)
425 antibody (R&D systems) at 1:10; or a rabbit monoclonal anti human LC3a/b (Light Chain 3,
426 autophagy marker) antibody (Cell Signaling Tech #12741S) used at 1:100. After removal of the
427 primary antibody, two washes in PBS and three washes in PBS with 3% BSA, cells were incubated
428 with fluor-conjugated secondary antibodies when applicable at 1:500 (Goat anti-Rabbit IgG (H+L)
429 secondary antibody, Alexa Fluor 488; 1:500 dilution) for 1 hour at room temperature. After brief
430 washing, cells were mounted with Vectashield Antifade mounting medium with DAPI (Fisher
431 Scientific) and immediately imaged using a Keyence all-in-one Fluorescence microscope camera
432 and Keyence software.

433 *T cell and selected CD4+ and CD8+ T cell secretion of IFN-γ in response to MoDCs pulsed with*
434 *SARS-CoV-2 peptide antigen pools*

435 The ability of T cells from previously infected patients used in these studies to recognize
436 SARS-CoV-2 antigens *in vitro* was validated and then similar analyses were performed for
437 selected CD4+ and CD8+ T cells. Briefly, MoDC (2 x 10^4) were pulsed with SARS-CoV-2 peptide
438 antigens (1μg/ml, PepMix S comprising the S1 and S2 pools PM-WCPV-S-1; and N PM-WCPV-
439 NCAP-1, both JPT Peptide Technologies) then autologous T cells (1 x 10^5), enriched from the
440 non-adherent fraction of PBMC using MojoSort (BioLegend CD3 enrichment) were added in
441 enriched RPMI (10% human AB serum). Cells were cultured in a microtiter plate (Millipore)
442 containing an immobilized primary antibody to target IFN-γ, overnight (37°C), then IFN-γ spot
443 forming cells enumerated by ELISpot. For ELISpot detection, after aspiration and washing to
444 remove cells and media, IFN-γ was detected by a secondary antibody to cytokine conjugated to
445 biotin. A streptavidin/horseradish peroxidase conjugate was used detect the biotin-conjugated

446 secondary antibody. The number of spots per well (1 x 10^5 cells), was counted using an ELISpot
447 plate reader. IL-4 was measured by ELISpot using a kit (MabTech) with wells precoated with anti-
448 IL-4 antibody and following the manufacturer's instructions. Remaining steps for IL-4 detection
449 were identical to those for IFN-γ, but with alkaline phosphatase detection rather than peroxidase.
450 *Determination of previously SARS-CoV-2 infected patient-derived T-cell reactivity in response to*
451 *autologous hAd5 vaccine-transduced MoDCs*
452 MoDCs were transduced with hAd5 S-Fusion, S-Fusion + N-ETSD, N-ETSD, N or GFP/Null
453 constructs and incubated overnight at 37°C. The transduced MoDCs were cultured with CD3+,
454 CD4+, or CD8+ T-cells from the same individuals overnight. Antigen specific T-cell responses
455 were enumerated using ELISpot as described above.
456
457 **Phase 1b Clinical Trail and Analyses**
458 *Vaccination of healthy adult subjects with hAd5-S-Fusion+N-ETSD.*
459 The cGMP vaccine used in the clinical trial was prepared using the generated high titer
460 adenoviral stocks described above in *Production hAd5-S-Fusion+N-ETSD and related SARS-*
461 *CoV-2 antigen expressing vectors*.
462 In a phase 1b, open-label study (QUILT 4.001 in adults conducted at Hoag Hospital in
463 Orange County, California, USA, hAd5-S-Fusion+N-ETSD was administered to cohort 2, the
464 participants evaluated in the studies here, subcutaneously at a dosage of $1x10^{11}$ VP. An initial
465 priming dose was administered on Day 1.
466 Study participants comprised healthy adult volunteers between the ages of 18 and 55. Subjects
467 were randomized to cohorts described above. All the participants provided informed, written
468 consent before enrollment.
469
470

471 *Trial Oversight*

472 The trial protocol was approved by the Western IRB for the Chan Soon-Shiong Institute for
473 Medicine (CSSIFM) and the Hoag Hospital Providence IRB at Hoag Hospital Newport Beach.
474 ImmunityBio, Inc. was the regulatory sponsor of the trial and holder of the Investigational New
475 Drug (IND) application. The trial was funded by ImmunityBio, Inc.. The vaccine was designed by
476 ImmunityBio, Inc. and manufacture by ImmunityBio. *The studies presented here are experimental*
477 *and all assays and analyses were performed in-house at ImmunityBio, Inc. Formal analyses of the*
478 *primary and secondary end points are not reported in this manuscript.*

479 *T-cell analyses*

480 T-cell responses in PBMCs were measured at baseline (Day 1) and after prime vaccination
481 alone on Day 14-16 and 21-23 by ELISpot for secretion of interferon γ (IFNγ) and interleukin 4
482 (IFN-4). T helper cell type 1 dominance was determined based on the IFNγ/IL-4 ratio.

483 *IFN-γ ELISpot for enumeration of S- and N-specific T cells in PBMC*

484 ELISpot assays were used to enumerate S- and N-specific IFN-γ-secreting T cells in fresh
485 PBMCs isolated from the blood of subjects vaccinated with hAd5-S-Fusion+N-ETSD. Whole
486 blood was collected by venipuncture pre- and post-vaccination. PBMCs were isolated from whole
487 blood by standard density gradient centrifugation and frozen in liquid nitrogen until use. On the
488 day of assay, PBMCs were thawed and re-suspended in RPMI 10% human AB serum, then
489 incubated with 2 μg/ml of SARS-CoV-2 S or N peptide pools (JPT Peptide Technologies catalogue
490 # PM-WCPV-S and PM-WCPV-NCAP-1, respectively). Internal positive controls were incubated
491 with 2 μg/ml of CEFT peptide pool consisting of epitopes derived from human Cytomegalovirus,
492 Epstein-Barr virus, Influenza A, and Clostridium tetani (JPT Peptide Technologies catalogue #
493 PM-CEFT-4). Positive assay controls were incubated with a CD3/CD28/CD2 agonist (StemCell
494 Technologies catalogue # 10970). Negative controls were incubated with media alone or 2 μg/ml

495 of SARS-CoV-2 membrane peptide pool (JPT Peptide Technologies catalogue # PM-WCPV-
496 VME). The number of spot-forming cells (SFCs) per well (2.5-4 x 10^5 PBMCs) were enumerated
497 using an ELISpot plate reader (Cellular Technologies Limited model # S6UNIV-01-7115). All
498 IFN-γ ELISpot reagents were obtained from a commercial kit and used according to manufacturer
499 protocol (Cellular Technologies Limited catalogue # Hu IFN-g/IL-4).
500

501 ***In silico* T-Cell Epitope HLA Binding Prediction**

502 *SARS-CoV-2 reference sequences*

503 The reference strain and COVID19 variants used for epitope analysis was assembled from
504 75,000 individual sequences deposited in the GISAID database. Binding analysis was run on the
505 consensus sequence generated using our in-house binding algorithm.[51] Briefly, machine learning
506 classifiers were trained on experimental binding data deposited in the IEDB database.[52]

507 The variants assessed included (name/mutation(s)): B.1.177/A222V mutation; B.1.1.7
508 /N501Y mutation; B.1.351 and B.1.1.28/K417N (or K417T for B.1.1.28), E484K, and the N501Y
509 mutations; and P.2/E484K. Binding efficiencies as well as HLA-epitope pairs were compared
510 between reference sequences and mutations to determine potential immune evasion due to the
511 reported variants.
512

513 **REFERENCES**

514 1 Gabitzsch, E. *et al.* Complete Protection of Nasal and Lung Airways Against SARS-
515 CoV-2 Challenge by Antibody Plus Th1 Dominant N- and S-Specific T-Cell Responses
516 to Subcutaneous Prime and Thermally-Stable Oral Boost Bivalent hAd5 Vaccination in
517 an NHP Study. *bioRxiv*, 2020.2012.2008.416297, doi:10.1101/2020.12.08.416297
518 (2021).
519 2 Amalfitano, A. Next-generation adenoviral vectors: new and improved. *Gene Therapy* **6**,
520 1643-1645, doi:10.1038/sj.gt.3301027 (1999).
521 3 Gabitzsch, E. S. & Jones, F. R. New recombinant SAd5 vector overcomes Ad5 immunity
522 allowing for multiple safe, homologous, immunizations. *J Clin Cell Immunol* **S4**, 001,
523 doi:doi:10.4172/2155-9899 (2011).

4 Gabitzsch, E. S. *et al.* Anti-tumor immunotherapy despite immunity to adenovirus using a novel adenoviral vector Ad5 [E1-, E2b-]-CEA. *Cancer Immunology, Immunotherapy* **59**, 1131-1135, doi:10.1007/s00262-010-0847-8 (2010).

5 Gatti-Mays, M. E. *et al.* A Phase I Trial Using a Multitargeted Recombinant Adenovirus 5 (CEA/MUC1/Brachyury)-Based Immunotherapy Vaccine Regimen in Patients with Advanced Cancer. *Oncologist* **25**, 479, doi:10.1634/theoncologist.2019-0608 (2019).

6 Hellerstein, M. What are the roles of antibodies versus a durable, high quality T-cell response in protective immunity against SARS-CoV-2? *Vaccine X* **6**, 100076, doi:10.1016/j.jvacx.2020.100076 (2020).

7 Redd, A. D. *et al.* CD8+ T cell responses in COVID-19 convalescent individuals target conserved epitopes from multiple prominent SARS-CoV-2 circulating variants. *Open Forum Infect Dis*, doi:10.1093/ofid/ofab143 (2021).

8 NIH. T cells recognize recent SARS-CoV-2 variants. *News Release* **https://www.nih.gov/news-events/news-releases/t-cells-recognize-recent-sars-cov-2-variants** (2021).

9 Tarke, A. *et al.* Negligible impact of SARS-CoV-2 variants on CD4+ and CD8+ T cell reactivity in COVID-19 exposed donors and vaccinees. *bioRxiv*, 2021.2002.2027.433180, doi:10.1101/2021.02.27.433180 (2021).

10 Baden, L. R. *et al.* Efficacy and Safety of the mRNA-1273 SARS-CoV-2 Vaccine. *N Engl J Med* **384**, 403-416, doi:10.1056/NEJMoa2035389 (2021).

11 Polack, F. P. *et al.* Safety and Efficacy of the BNT162b2 mRNA Covid-19 Vaccine. *N Engl J Med* **383**, 2603-2615, doi:10.1056/NEJMoa2034577 (2020).

12 Sadoff, J. *et al.* Interim Results of a Phase 1-2a Trial of Ad26.COV2.S Covid-19 Vaccine. *N Engl J Med*, doi:10.1056/NEJMoa2034201 (2021).

13 Ewer, K. J. *et al.* T cell and antibody responses induced by a single dose of ChAdOx1 nCoV-19 (AZD1222) vaccine in a phase 1/2 clinical trial. *Nat Med* **27**, 270-278, doi:10.1038/s41591-020-01194-5 (2021).

14 Keech, C. *et al.* Phase 1-2 Trial of a SARS-CoV-2 Recombinant Spike Protein Nanoparticle Vaccine. *N Engl J Med* **383**, 2320-2332, doi:10.1056/NEJMoa2026920 (2020).

15 Anderson, E. J. *et al.* Safety and Immunogenicity of SARS-CoV-2 mRNA-1273 Vaccine in Older Adults. *N Engl J Med* **383**, 2427-2438, doi:10.1056/NEJMoa2028436 (2020).

16 Sahin, U. *et al.* COVID-19 vaccine BNT162b1 elicits human antibody and T(H)1 T cell responses. *Nature* **586**, 594-599, doi:10.1038/s41586-020-2814-7 (2020).

17 Karim, S. S. A. Vaccines and SARS-CoV-2 variants: the urgent need for a correlate of protection. *The Lancet*, doi:10.1016/S0140-6736(21)00468-2.

18 Madhi, S. A. *et al.* Efficacy of the ChAdOx1 nCoV-19 Covid-19 Vaccine against the B.1.351 Variant. *New England Journal of Medicine*, doi:10.1056/NEJMoa2102214 (2021).

19 Shinde, V. *et al.* Preliminary Efficacy of the NVX-CoV2373 Covid-19 Vaccine Against the B.1.351 Variant. *medRxiv*, 2021.2002.2025.21252477, doi:10.1101/2021.02.25.21252477 (2021).

20 Novavax. Novavax COVID-19 Vaccine Demonstrates 89.3% Efficacy in UK Phase 3 Trial. (2021).

21 Johnson, J. Johnson & Johnson Announces Single-Shot Janssen COVID-19 Vaccine Candidate Met Primary Endpoints in Interim Analysis of its Phase 3 ENSEMBLE Trial. (2021).

22 Edara, V. V. *et al.* Reduced binding and neutralization of infection- and vaccine-induced antibodies to the B.1.351 (South African) SARS-CoV-2 variant. *bioRxiv*, doi:10.1101/2021.02.20.432046 (2021).
23 Wang, Z. *et al.* mRNA vaccine-elicited antibodies to SARS-CoV-2 and circulating variants. *Nature* **Preview**, doi:10.1038/s41586-021-03324-6 (2021).
24 Wu, K. *et al.* mRNA-1273 vaccine induces neutralizing antibodies against spike mutants from global SARS-CoV-2 variants. *bioRxiv*, doi:10.1101/2021.01.25.427948 (2021).
25 Azizi, A. *et al.* A combined nucleocapsid vaccine induces vigorous SARS-CD8+ T-cell immune responses. *Genet Vaccines Ther* **3**, 7, doi:10.1186/1479-0556-3-7 (2005).
26 Shang, B. *et al.* Characterization and application of monoclonal antibodies against N protein of SARS-coronavirus. *Biochemical and Biophysical Research Communications* **336**, 110-117, doi:https://doi.org/10.1016/j.bbrc.2005.08.032 (2005).
27 Peng, H. *et al.* Long-lived memory T lymphocyte responses against SARS coronavirus nucleocapsid protein in SARS-recovered patients. *Virology* **351**, 466-475, doi:https://doi.org/10.1016/j.virol.2006.03.036 (2006).
28 Narayanan, K., Chen, C.-J., Maeda, J. & Makino, S. Nucleocapsid-independent specific viral RNA packaging via viral envelope protein and viral RNA signal. *Journal of virology* **77**, 2922-2927, doi:10.1128/jvi.77.5.2922-2927.2003 (2003).
29 Zeng, W. *et al.* Biochemical characterization of SARS-CoV-2 nucleocapsid protein. *Biochemical and biophysical research communications*, S0006-0291X(0020)30876-30877, doi:10.1016/j.bbrc.2020.04.136 (2020).
30 Grifoni, A. *et al.* Targets of T Cell Responses to SARS-CoV-2 Coronavirus in Humans with COVID-19 Disease and Unexposed Individuals. *Cell* **181**, 1489, doi:10.1016/j.cell.2020.05.015 (2020).
31 Le Bert, N. *et al.* SARS-CoV-2-specific T cell immunity in cases of COVID-19 and SARS, and uninfected controls. *Nature* **584**, 457, doi:10.1038/s41586-020-2550-z (2020).
32 Sekine, T. *et al.* Robust T cell immunity in convalescent individuals with asymptomatic or mild COVID-19. *Cell* **183**, 158, doi:10.1101/2020.06.29.174888 (2020).
33 Altmann, D. M. & Boyton, R. J. SARS-CoV-2 T cell immunity: Specificity, function, durability, and role in protection. *Sci Immunol* **5**, eabd6160, doi:10.1126/sciimmunol.abd6160 (2020).
34 Chen, Z. & John Wherry, E. T cell responses in patients with COVID-19. *Nat Rev Immunol*, 1-8, doi:10.1038/s41577-020-0402-6 (2020).
35 Matloubian, M., Concepcion, R. J. & Ahmed, R. CD4+ T cells are required to sustain CD8+ cytotoxic T-cell responses during chronic viral infection. *Journal of virology* **68**, 8056-8063, doi:10.1128/jvi.68.12.8056-8063.1994 (1994).
36 Laidlaw, B. J., Craft, J. E. & Kaech, S. M. The multifaceted role of CD4(+) T cells in CD8(+) T cell memory. *Nat Rev Immunol* **16**, 102-111, doi:10.1038/nri.2015.10 (2016).
37 Nakamura, S. & Yoshimori, T. New insights into autophagosome-lysosome fusion. *J Cell Sci* **130**, 1209-1216, doi:10.1242/jcs.196352 (2017).
38 Lőrincz, P. & Juhász, G. Autophagosome-Lysosome Fusion. *J Mol Biol* **432**, 2462-2482, doi:10.1016/j.jmb.2019.10.028 (2020).
39 Kabeya, Y. *et al.* LC3, a mammalian homologue of yeast Apg8p, is localized in autophagosome membranes after processing. *Embo j* **19**, 5720-5728, doi:10.1093/emboj/19.21.5720 (2000).
40 Schmid, D., Pypaert, M. & Münz, C. Antigen-loading compartments for major histocompatibility complex class II molecules continuously receive input from autophagosomes. *Immunity* **26**, 79-92, doi:10.1016/j.immuni.2006.10.018 (2007).

619 41 Patterson, N. L. & Mintern, J. D. Intersection of autophagy with pathways of antigen
620 presentation. *Protein & Cell* **3**, 911-920, doi:10.1007/s13238-012-2097-3 (2012).
621 42 Crotzer, V. L. & Blum, J. S. Autophagy and Its Role in MHC-Mediated Antigen
622 Presentation. *The Journal of Immunology* **182**, 3335, doi:10.4049/jimmunol.0803458
623 (2009).
624 43 You, L. *et al.* The crosstalk between autophagic and endo-/exosomal pathways in antigen
625 processing for MHC presentation in anticancer T cell immune responses. *Journal of*
626 *Hematology & Oncology* **10**, 165, doi:10.1186/s13045-017-0534-8 (2017).
627 44 Tan, C. W. *et al.* A SARS-CoV-2 surrogate virus neutralization test based on antibody-
628 mediated blockage of ACE2-spike protein-protein interaction. *Nat Biotechnol* **38**, 1073-
629 1078, doi:10.1038/s41587-020-0631-z (2020).
630 45 GISAID. SARS-CoV-2 Lineages. (2020-2021).
631 46 Peng, Y. *et al.* Broad and strong memory CD4(+) and CD8(+) T cells induced by SARS-
632 CoV-2 in UK convalescent individuals following COVID-19. *Nat Immunol* **21**, 1336-
633 1345, doi:10.1038/s41590-020-0782-6 (2020).
634 47 Rice, A. *et al.* The Dual-Antigen Ad5 COVID-19 Vaccine Delivered as an Intranasal Plus
635 Subcutaneous Prime Elicits Th1 Dominant T-Cell and Humoral Responses in CD-1 Mice.
636 *bioRxiv*, 2021.2003.2022.436476, doi:10.1101/2021.03.22.436476 (2021).
637 48 Tilocca, B. *et al.* Comparative computational analysis of SARS-CoV-2 nucleocapsid
638 protein epitopes in taxonomically related coronaviruses. *Microbes Infect*, S1286-
639 4579(1220)30053-30058, doi:10.1016/j.micinf.2020.04.002 (2020).
640 49 Amalfitano, A. *et al.* Production and Characterization of Improved Adenovirus Vectors
641 with the E1, E2b, and E3 Genes Deleted. *Journal of virology* **72**, 926,
642 doi:10.1128/JVI.72.2.926-933.1998 (1998).
643 50 Kasinrerk, W., Baumruker, T., Majdic, O., Knapp, W. & Stockinger, H. CD1 molecule
644 expression on human monocytes induced by granulocyte-macrophage colony-stimulating
645 factor. *The Journal of Immunology* **150**, 579-584 (1993).
646 51 Elbe, S. & Buckland-Merrett, G. Data, disease and diplomacy: GISAID's innovative
647 contribution to global health. *Glob Chall* **1**, 33-46, doi:10.1002/gch2.1018 (2017).
648 52 Vita, R. *et al.* The Immune Epitope Database (IEDB): 2018 update. *Nucleic Acids Res* **47**,
649 D339-d343, doi:10.1093/nar/gky1006 (2019).
650 53 Tan, C. W. *et al.* A SARS-CoV-2 surrogate virus neutralization test based on antibody-
651 mediated blockage of ACE2-spike protein-protein interaction. *Nat Biotechnol* **38**, 1973,
652 doi:10.1038/s41587-020-0631-z (2020).
653

654

655

656

657

658

659

660

661 **SUPPLEMENTARY MATERIALS for**
662
663 **Single Prime hAd5 Spike (S) + Nucleocapsid (N) Dual Antigen Vaccination of**
664 **Healthy Volunteers Induces a Ten-Fold Increase in Mean S- and N- T-Cell Responses**
665 **Equivalent to T-Cell Responses from Patients Previously Infected with SARS-CoV-2**
666
667 **Supplementary Materials**
668
669 **Methods**
670
671 *Quantification of anti-SARS-CoV-2 spike antibodies in plasma*
672
673 The presence of anti-SARS-CoV-2 spike antigen antibodies in previously infected patient
674 plasma used in studies here was validated. IgG against SARS-CoV-2 spike was detected in plasma
675 using ELISA. Briefly, EIA/RIA plates were coated with a solution of purified recombinant SARS-
676 CoV-2-derived Spike protein (1μg/ml, S-Fusion. ImmunityBio, Inc.) suspended in coating buffer
677 (0.05 M carbonate-bicarbonate, pH 9.6) and incubated overnight at 4°C. Plates were washed three
678 times with TPBS solution (PBS + 0.05% Tween 20). Blocking solution (2% non-fat milk in TPBS)
679 was added and incubated at room temperature (RT, 1h). Serial dilutions of plasma were prepared
680 in 1% non-fat milk in TPBS. Plates were washed as described above and serial dilutions of plasma
681 were added to the plate and incubated at RT (1h). Plates were washed three times. Goat anti-
682 Human IgG (H+L) HRP-conjugated secondary antibody (1:6000 dilution) prepared in 1% non-fat
683 milk/TPBS was added and incubated at RT (1h). Plates were washed three times. Substrate
684 (3,3',5,5'-tetramethylbenzidine (TMB)) was added to each well and incubated at RT (10min). The
685 reaction was stopped by addition of sulfuric acid (1N H_2SO_4). The optical density (450 nm) was
686 measured by a Synergy 2 (BioTek Instruments, Inc.) plate reader. Data were analyzed using Prism
687 8 (GraphPad Software, LLC).
688
689 *cPass™ neutralizing antibody detection*
690
691 The GenScript cPass™ (https://www.genscript.com/cpass-sars-cov-2-neutralization-
692 antibody-detection-Kit.html) kit for detection of neutralizing antibodies was used according to the
693 manufacturer's instructions.[44] The kit detects circulating neutralizing antibodies against SARS-
694 CoV-2 that block the interaction between the S RBD with the ACE2 cell surface receptor. It is
695 suitable for all antibody isotypes.
696
697 To evaluate the levels of anti-SARS-CoV-2 neutralizing antibodies in plasma, dilutions of
698 plasma were incubated with horseradish peroxidase-conjugated spike RBD (37°C, 30min). The
699 RBD-plasma mixture was added to a microtiter plate coated with ACE2 and incubated at 37°C (15
700 min). Plates were washed and substrate (TMB) added at room temperature (15 min). The reaction
701 was stopped and plates read on a plate reader at 450 nm.
702
703 *Live virus assay of plasma neutralization of infection*
704
705 The ability of previously SARS-CoV-2 infected patient plasma used in studies here to
706 neutralize SARS-CoV-2 infection *in vitro* was also validated. All aspects of the assay utilizing
707 virus were performed in a BSL3 containment facility according to the ISMMS Conventional
708 Biocontainment Facility SOPs for SARS-CoV-2 cell culture studies. Vero E6 kidney epithelial
709 cells from *Cercopithecus aethiops* (ATCC CRL-1586) were plated (20,000 cells/well) in a 96-well

710 format and 24 hours later, cells were incubated with antibodies or heat inactivated plasma
711 previously serially diluted in 3-fold steps in DMEM containing 2% FBS, 1% NEAAs, and 1%
712 Pen-Strep; the diluted samples were mixed 1:1 with SARS-CoV-2 in DMEM containing 2% FBS,
713 1% NEAAs, and 1% Pen-Strep at 10,000 TCID 50/mL for 1 hr at 37ºC, 5% CO_2. This incubation
714 did not include cells to allow for neutralizing activity to occur prior to infection. For detection of
715 neutralization, the virus/sample mixture (120 µL) was transferred to the Vero E6 cells and
716 incubated (48 hours) before fixation with 4% PFA. Each well received virus (60 µl) or an infectious
717 dose of 600 TCID50. Control wells, including six wells on each plate for no virus and virus-only
718 controls, were used. The percent neutralization was calculated as 100-((sample of interest-[average
719 of "no virus"])/[average of "virus only"])*100) with a stain for CoV-2 Np imaged on a Celigo
720 Imaging Cytometer (Nexcelom Bioscience).
721
722 *Transfection of HEK 293T cells and detection of plasma antibody binding*
723
724 To assess binding of plasma from a previously infected patient to antigens expressed by hAd5
725 S-Fusion and hAd5 S-Fusion + N-ETSD vaccines, plasma was incubated with construct-
726 transfected HEK 293T cells and binding determined by flow cytometry. HEK 293T cells (2.5 x
727 10^5 cells/well in 24 well plates) were grown in DMEM (Gibco) with 10% FBS and 1X PSA (100
728 units/mL penicillin, 100 µg/mL streptomycin, 0.25 µg/mL Amphotericin B) at 37ºC. Cells were
729 either left untransfected or were transfected with 0.5 µg of S-Fusion or S-Fusion + N-ETSD hAd5
730 plasmid DNA using a JetPrime transfection reagent (Polyplus) according to the manufacturer's
731 instructions. Twenty-four hours later, cells were incubated for 30 min. with previously infected
732 patient or healthy (unexposed, UnEx) plasma that had been serially diluted 10-fold for 30 min.
733 Plasma IgG was labeled using a goat anti-human IgG-phycoerythrin conjugated and labeled cells
734 were acquired using the Thermo-Fisher Attune NxT flow cytometer and analyzed using FlowJo
735 Software to determine Mean Fluorescence Intensity (MFI) values of both the untransfected and
736 transfected cells. Results were graphed as the difference in MFI between untransfected and
737 transfected cells for the S-Fusion and S-Fusion + N-ETSD constructs over the plasma dilutions.
738
739 **Results**
740
741 *Previously SARS-CoV-2-infected patient plasma confirmed to have neutralizing anti-S antibodies*
742
743 For the studies described below, plasma samples were collected from four individuals
744 convalescing from SARS-CoV-2 infection as confirmed by antibody assays and patient history as
745 described Methods. The presence of anti-Spike IgG, and of neutralizing antibodies by both a
746 surrogate SARS-CoV-1 neutralization assay [53] and live virus assays, were confirmed in all patient
747 samples (Suppl. Fig. S1**).** Samples were also collected from four virus-naïve individuals and were
748 used as controls.

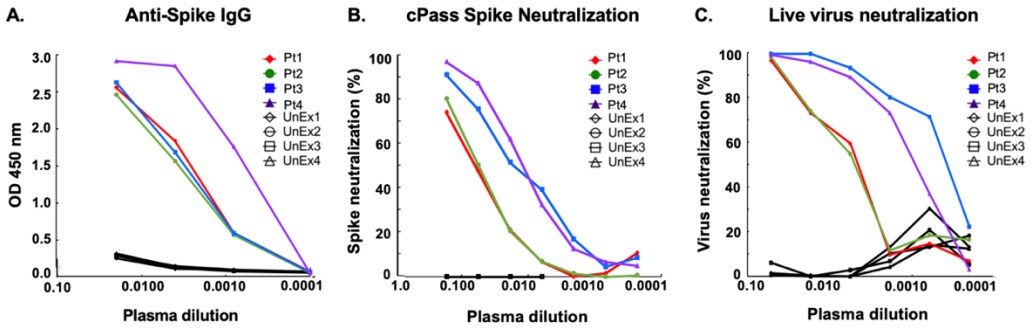

749

750 **Fig. S1** *Plasma samples from patients (Pt) previously infected with SARS-CoV-2 contain*
751 *neutralizing antibodies*. (A) The levels of anti-spike IgG as determined by OD at 450 nm are
752 shown. (B) All four Pt plasma samples contained antibodies that blocked RBD-ACE2 binding and
753 (C) contained SARS-CoV-2 neutralizing antibodies.
754 *Previously SARS-CoV-2-infected patient plasma binds to vaccine-transfected HEK-293T cells*
755
756 In additional studies to validate immune responses to SARS-CoV-2 antigens, the binding of
757 previously SARS-CoV-2 infected patient and virus-naïve control individual plasma to human
758 embryonic kidney (HEK) 293T cells transfected with either hAd5 S-Fusion alone or hAd5 S-
759 Fusion + N-ETSD was assessed (Suppl. Fig. S2). This binding reflects the presence of antibodies
760 in plasma that recognize antigens expressed by the hAd5 vectored vaccines. Quantification of
761 histograms showed little or no binding of virus-naïve plasma antibodies to cells expressing either
762 construct, and the highest binding of plasma antibodies from a previously SARS-CoV-2 infected
763 patient to cells expressing the dual antigen S-Fusion + N-ETSD construct (Suppl. Fig. S2R**).**

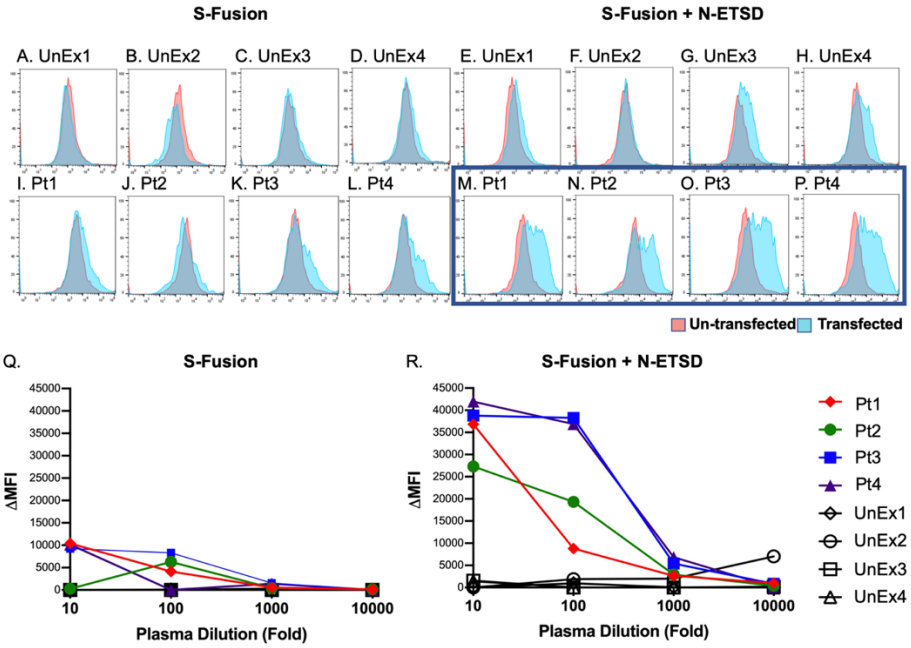

764
765 **Fig. S2** *Plasma from previously SARS-CoV-2 infected patients shows greater binding to S-Fusion*
766 *+ N-ETSD surface antigens compared to S-Fusion alone after transfection of HEK 293T cells*.
767 HEK 293T cells that were either uninfected (pink) or infected (blue) with S-Fusion alone or
768 bivalent S-Fusion + N-ETSD were exposed to plasma from either unexposed (UnEx) controls or
769 previously infected SARS-CoV-2 patients (Pt). Flow histograms for (A-D) UnEx with S-Fusion;
770 (E-H) UnEx with S-Fusion + N-ETSD; (I-L) Pt with S-Fusion; and (M-P) Pt with S-Fusion + N-
771 ETSD, all n = 4, are shown. When the ΔMFI (difference in binding to transfected versus
772 untransfected cells) is graphed, it is apparent that compared to (Q) S-Fusion, (R) binding of Pt
773 plasma to S-Fusion + N-ETSD transfected cells is much higher and that plasma from UnEx
774 individuals shows little binding.
775
776 *Previously SARS-CoV-2-infected patient T cells are activated by S and N peptide pools*
777
778 The reactivities of T cells from the previously SARS-CoV-2-infected patients was confirmed
779 by incubation with S1 (containing the spike receptor binding domain), S2 and N peptides pools

780 (Fig. S3A). The specific reactivities of CD4+ (Fig. S3B and C) and CD8+ T cells was then
781 determined, showing CD8+ T cells were more selectively activated by the N peptide pool.
782

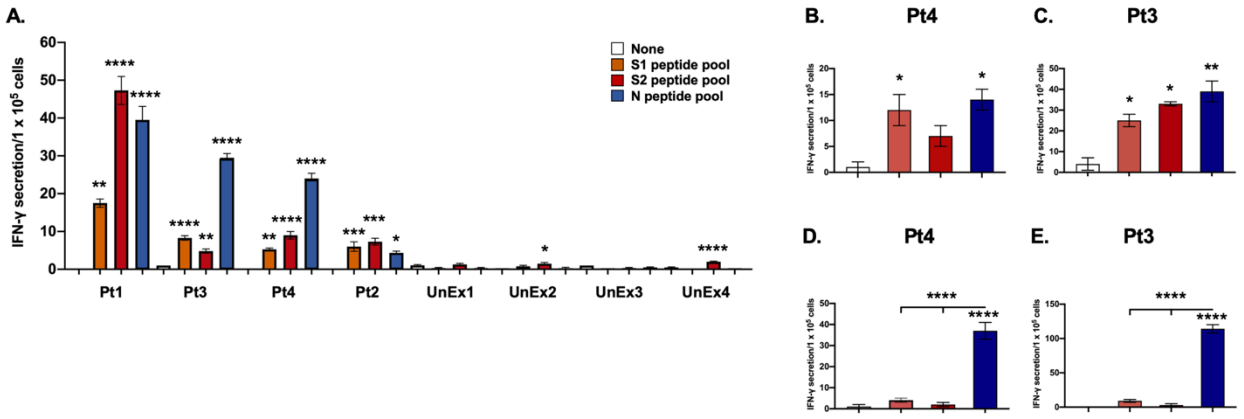

783

784 **Fig. S3.** *T-cell responses to MoDCs pulsed with SARS-CoV-2 peptides.* Unselected T cells from
785 all four previously SARS-CoV-2 infected patients (Pt) show significant IFN-γ responses to S1, S2,
786 and N peptide pool-pulsed MoDCs as compared to 'none'. T cells from virus-naïve (unexposed,
787 UnEx) control individuals showed far lower responses. Statistical analysis performed using One-
788 way ANOVA and Tukey's post-hoc analysis for samples from each patient compared only to
789 'none' where * p<= 0.05, **p<0.01, ***p<0.001, and ****p<0.0001. Data graphed as the mean
790 and SEM; n = 3-4. Patient MoDCs pulsed with SARS-CoV-2 peptide mixes overnight were
791 incubated with autologous CD4+ (B, Pt 4; C, Pt 3) or CD8+ (D, Pt 4; E, Pt 3) T cells. IFN-γ levels
792 were determined by ELISpot. Statistical analysis performed using One-way ANOVA and
793 Dunnett's post-hoc multiple comparison analysis to compare each peptide pool to Veh (shown
794 above the bar) or between peptide pools (above line) where *p<0.05, **p<0.01 and
795 ****p<0.00001. Data graphed as mean and SEM; n = 3.